Energy Efficient DC-Grids for Commercial Buildings

Bernd Wunder, Fraunhofer Institut IISB, Germany
Leopold Ott, Fraunhofer Institut IISB, Germany
Marek Szpek, Emerson Network Power, Sweden
Ulrich Boeke, Philips Electronics Netherland B.V., Philips Research, the Netherlands
Dr. Roland Weiß, Siemens AG, Corporate Technology, Germany

***Abstract* - Modern power electronics enable the efficient supply of almost all kinds of electric applications in commercial buildings, e. g. lighting, IT- and telecommunication equipment, as well as speed-controlled drives in heating, cooling and ventilation applications. This potential can be used more effectively using a 380 V_{DC} Grid compared to a traditional AC Grid in commercial buildings.**

The European ENIAC R&D project consortium DC Components and Grid (DCC+G) is developing suitable, highly efficient components and sub systems for 380 V_{DC} grid to show the benefits of DC grid concept on test site in an office environment. The newly developed DC Grid components and their integration into a generic system are presented in this paper. The targeted overall efficiency saving compared to AC grid is 5% and the energy conversion from PV is calculated to be 7% higher compared to traditional PV inverter conversion. This paper also shows the layout of the office demonstrator at Fraunhofer Institute in Erlangen, Germany, and describes general benefits of a DC Grid system.

I. POTENTIAL OF MODERN POWER ELECTRONICS IN DC GRIDS

In the last decade research and development work in the field of power electronic semiconductor lead among other things to following improvements:

- Significant reduction of conduction losses (R_{DSON}) in power electronic devices, through technologies like Trench MOSFET technology [1], super junction technology [2], [3] and upcoming technologies like Multiple Epitaxy and Deep Trench [4].
- Steadily increasing switching performance and reduction of parasitic capacitances in power electronic devices.
- Application of new devices on basis of wide band gap semiconductor materials (SiC and GaN) with advanced switching and temperature performance [5].

An important benefit of the new ultra-fast switching devices is the possibility to increase the operation frequency in the power electronic circuits and shrink down passive components size to get higher power density in many applications. This lead also to a reduction of the application costs because the passive component size is correlated to the costs. These trends and the improvements in power density and efficiency over the last years in the research and industry area are described in [6]-[9].

As an example, a switch mode power supply for a flat TV screen is shown in figure 1. According to [10], [11] approximately 50 % of losses, 70% of weight and 70 % of volume are necessary for the rectifier, EMI filter, power factor correction and DC link storage. This means that most of the cost, volume and efficiency of the power supply is wasted in the AC line front-end with the only task to provide a DC (link) voltage. The really bad story is that we do this in almost every electronic device. Several times on an office desk, in driver for LED lamps and in many consumer electronics.

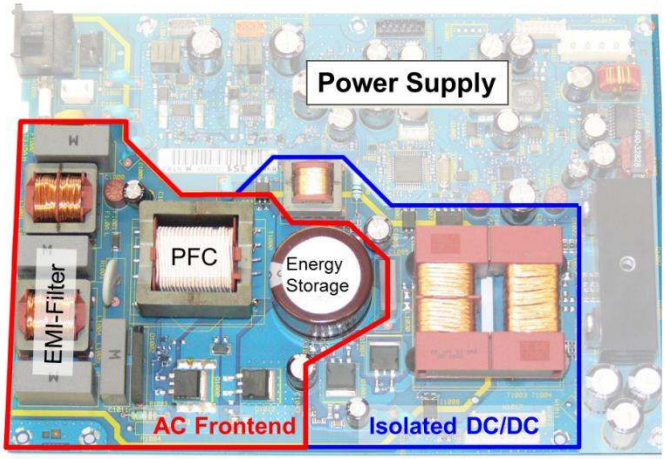

Figure 1: Different parts of a typical power supply for a flat TV as described in [10] and [11].

In more and more applications it is possible to develop integrated power electronic solutions. Moore's law predicts the number of transistors in a dense integrated circuit doubles approximately every two years. Integrated power electronic circuit can benefit from these improvements in semiconductor technologies. But in applications connected to a 50 Hz or 60 Hz AC grid, line frequency is fixed and the size of the passive filter components, power factor correction circuit and link capacitor cannot be further reduced. In that circuit area (marked red) there is only a small volume benefit through new faster switching devices and the usage of new semiconductor materials.

GaN devices (25A/100V) allow switching frequencies up to 10 MHz with 89% efficiency in size of a SO-8 package [12]-[14]. Optimized GaN driver and control circuits can provide efficiency up to 93 %

[14]. This means, that the blue marked area in figure 1 will be dramatically decrease in volume and costs over the next years.

DC micro grids can use the benefits of the new fast switching power electronic devices especially in power density, cost and efficiency issues. There is a trade of behavior between these three factors which allows the individual optimization for the applications.

II. THE RIGHT VOLTAGE LEVEL

ETSI EN 300 132-3-1 standard specifies a voltage range from 260 V_{DC} to 400 V_{DC} for a new DC interface for ICT equipment in telecom and data centers [15]. This wide voltage range has been selected with regard to power systems equipped with batteries. Nominal operating voltages in telecom and data centers are 354 V_{DC} and 380 V_{DC}, but when outage occurs, the battery voltage drops down to 260 V_{DC}.

However, variable battery voltages can be easily stabilized with a DC/DC converter. That is why DCC+G consortium has selected 380 V_{DC} ± 20 V voltage range for 380 V_{DC} loads and ±380 V_{DC} with ±20 V tolerance for 760 V_{DC} loads. This is a good compromise between highest achievable efficiency, available power semiconductors, compatibility with ETSI EN 300 132-3-1 and already existing power supplies for AC grids.

III. SWITCHED MODE POWER SUPPLY (SMPS)

Many applications in office environments operate with DC voltages equal or lower than 24 V, like computers, laptops, monitors, and printers. A rectifier, PFC stage and an isolating DC/DC converter (e.g. resonant (LLC) or Flyback type) are typically used to convert AC mains voltage into save low DC supply voltages.

A two stage topology for AC/DC adapters as shown in figure 2 and described in [16] can be divided into the AC rectifier and PFC stage forming the AC line front-end, and a DC/DC converter for generating the application specific extra low voltage. The line front-end generates a stable output voltage in the range of 380 V_{DC}. The second part provides the application voltage, for example 24 V_{DC}.

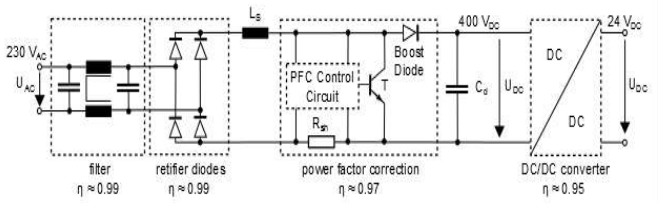

Figure 2: Different circuit blocks of a typical switch mode power supply to provide a voltage of 24 V.

One basic concept of the proposed 380 VDC grid is to centralize the AC line front-end (filter, rectifier, and power factor correction), i.e. each application device only needs the second stage (DC/DC converter). The central front-end for many devices can be more complex and more efficient because of higher power flow through it and it can also benefit of statistical and scale effects. Overall, this saves energy, costs, and material because the central rectifier can be optimized on a higher performance level compared to a small cost sensitive single AC/DC adapter. In addition, a large central rectifier can be designed to provide a variable power factor that would be too expensive for cost sensitive applications.

Another optimization can be the efficiency. The efficiency of the frontend converter in figure 2 is typically 95 %. The central rectifier of the DCC+G Project achieves an efficiency up to 97% over a wide load range [17]: i.e. 2% efficiency improvement with less electronic and costs in the application.

Low cost line adapters for external hard disks, mobile phones, battery chargers, USB hubs, and routers mostly have much lower efficiency in the range of 50-80 % [18]. For comparison, non-isolating DC/DC converters (24 V / 5 V) easily achieve efficiencies of 90-98 %, insulating DC/DC converters (380 V_{DC} / 24 V) efficiencies of 90-95 %.

Buildings which already have a photovoltaic system and/or battery storage installation have already a DC bus. So if there are sources that provide energy direct on the 380 V_{DC} grid the frontend losses of approximately 5 % can be avoided completely.

IV. OPTIMAL EMI FILTER DESIGN FOR 380 V_{DC}

Filter circuits for AC grid connected devices are optimized to comply with conducted emission requirements related to standards for the product that is selected. For IT/ICT equipment such a standard is IEC/EN 55022 and for lighting systems it is IEC/EN 55015. In the scope of DCC+G our goal is to provide at least the same DC Grid quality as on the AC side, so we specified the same EMI requirements for the DC grid.

As an example, a fluorescent lamp ballast is considered, with a similar topology as shown in figure 2. Instead of the DC/DC converter, the second stage is a resonant high frequency (50 kHz) DC/AC inverter in this application.

To characterize the EMI behavior we directly connected the DC/AC inverter of the lamp ballast to the 380 V_{DC} grid. Then measurements according to IEC/EN 55015 have been done [19].

Several measurements with different configurations of the driver have been made. The reference measurement was done on the complete AC circuit without the frontend filter. This is compared with the DC case where only the second stage (resonant DC/AC inverter) was used. These two cases are shown in figure 3. It can be seen that in the lower frequency range below 80 kHz the conducted noise voltages in the DC case are up to 40 dBµV lower as in the AC case. In the medium frequency range up to 3 MHz the DC case shows an approximately 10 dBµV higher noise level than the AC case. In the higher frequency range the DC case again shows better EMI properties.

The necessary DC-filter has to be optimized for higher middle frequency and a smaller bandwidth compared to the AC-filter. A filter for higher frequencies results in smaller foot print and less attenuation requirement. Thus the effort of such DC grid filter will be lower than for an AC grid filter.

Reference [20] mentions that a typically EMI input filter utilizes capacitors to provide a low impedance shunt path for high frequency currents. So such capacitors must be able to shunt current over a wide frequency range. To achieve this, various types of capacitors are placed in parallel. Large capacitance electrolytic capacitors are used to shunt lower frequencies and provide voltage holdup. For mid-range frequencies typical X-type and Y-type film and ceramic capacitors are employed [21].

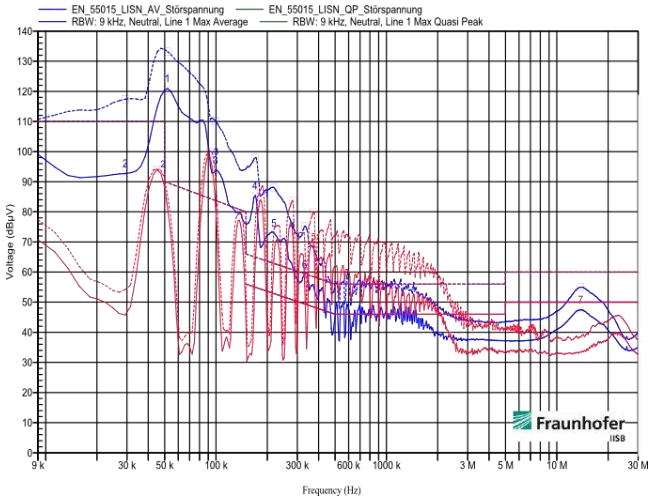

Figure 3: AC grid (blue) and DC grid (red) EMI behavior of a fluorescent lamp driver without filter (situation before filter design starts).

The better low frequency EMI performance allows smaller EMI filter capacitors and inductors in the DC case. The large capacitance electrolytic capacitors can also be reduced or even removed. The specification of a hold-up time in DC grids, e.g. for bridging arc extinction events, is still in discussion.

V. LIGHTING TEST BED INSTALLATIONS

Philips Research has realized a first LED lighting test bed installation with a 380 V_{DC} grid in Eindhoven, the Netherlands that is depicted in Figure 4. The installation makes use of 54 LuxSpace LED downlights (37 W each) that is a DC load of 2 kW. The LED downlight luminaires have been equipped with new LED drivers for a supply from 380 V_{DC}. The test bed has a hybrid supply from a 2 kW central rectifier as well as a 2 kW solar power system illustrated with Figure 5. For efficiency comparison a second lighting and solar system with an AC grid as well as several smart power meters have been installed.

The learning's from these installations are that, first, a trained technician can do a DC system installation with very little additional training. Second, the 2000 W central rectifier prototype is about 1% more efficient than a 39 W rectifier of a LED driver for 230 V_{AC} mains. Third, the 2 kW solar MPP converter prototype of the DC grid has a similar efficiency of about 97 % like the 12 kW 3-phase AC grid connected solar inverter. Hereby one has to take into account that the 12 kW solar inverter operates with a higher DC input voltage of typically 610 V_{DC} compared with 250 V_{DC} of the 2 kW MPP converter. Forth, the efficiency advantage of the DC grid system is as higher as more solar power is used due to less absolute losses in the central rectifier.

Figure 4: LED downlights powered from 380 V_{DC} at Philips Research in Eindhoven, the Netherlands.

Two additional LED lighting test bed installations are under preparation at Philips Research in Eindhoven, the Netherlands and at the Fraunhofer Institute IISB in Erlangen, Germany in 2014. The installations will have always two sub-systems with AC and DC grids to measure efficiency differences.

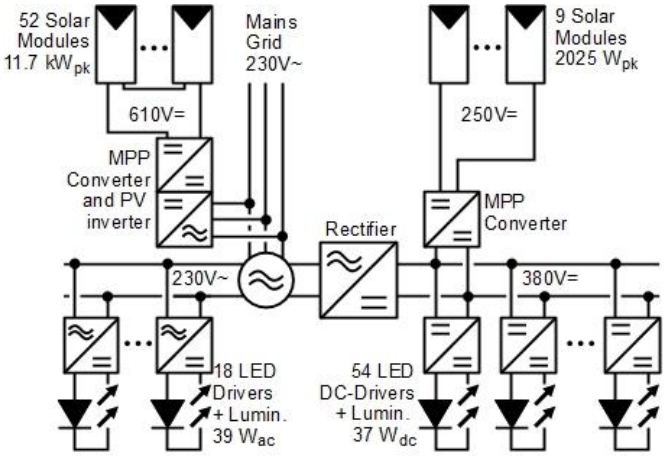

Figure 5: Philips 380 V_{DC} grid test bed with hybrid supply from solar power and utility mains.

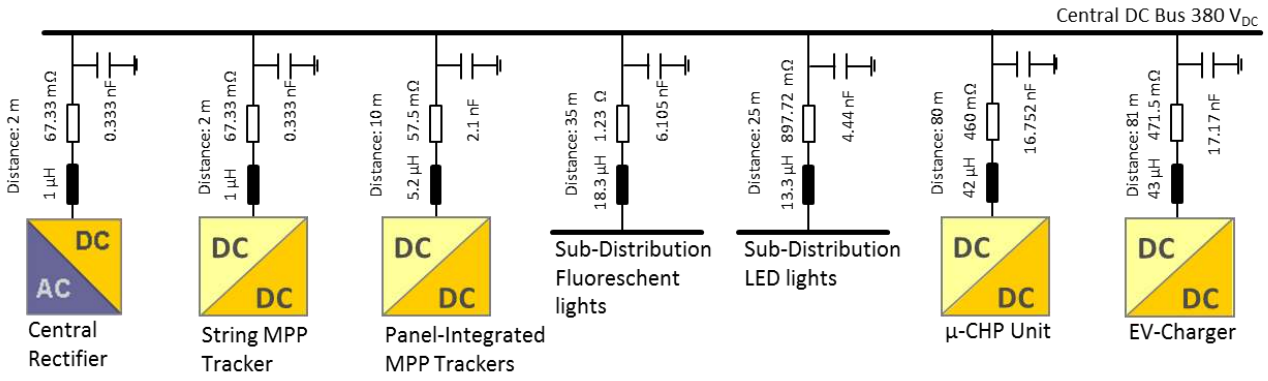

Figure 6: Cable modeling of office demonstrator. Main Power Modules of the DC Test Grid with specific connection impedance to the central DC bus. This model is used for stabilization analyses as reported in [24] and for efficiency calculations.

VI. CABLE MATERIAL SAVINGS AND EFFICIENCY INCREASE

In the office test bed at Fraunhofer Institute IISB in Erlangen the power system delivers two 380 V_{DC} phases with regulated output to the distribution network. The cable losses decreases because of a higher RMS voltage level (380 V_{DC}) and therefore the lower currents in the cables compared to conventional AC system (230 V_{AC}). With the same effective cross area section of the cables and a power factor of 1 the distribution losses decreases to 36.6 % compared to the AC case.

$$\frac{P_{DC}}{P_{AC}} = \frac{R_{Cable} \cdot (V_{AC})^2}{R_{Cable} \cdot (V_{DC})^2} = 0.366 \qquad (1)$$

But in a real AC grid the power factor is normally different to 1. These increases further the losses in an AC distribution. In a DC distribution grid the power factor is always 1.

In the DCC+G project the comparison of cable losses between a 2-phase ±380 V_{DC} and 3-phase 400 V_{AC} distribution is of special interest. Two typical situations are shown in [22]. Considering the same total cable conductor cross section the DC distribution has 58 % (resistive load) or 67 % (Non-linear load) lower losses compared to the equivalent AC distribution. These leads to a system level benefit for commercial buildings of about 2 % in the DC power cables [22].

Another possibility of a 380 V_{DC} distribution system is to upgrade already installed cables to a higher power level. This can be done because the limiting factor in the cables is generally not the voltage rating but the thermal behavior, which is mainly influenced by the current, cable and the ambient temperature.

In new installations this advantage can be used to reduce installation costs, and it also supports the saving of limited resources, like copper. With raising cost of copper as reported in [23] and increasing energy costs cable issues will put DC distribution systems in flavor for AC systems.

VII. STABILITY AND CABLE LENGTH

The complex cable impedance can influence the stability of grids. A "4G6" cable type is used in the DCC+G project to connect a micro-CHP unit and an electric vehicle charger to the central DC bus. For this cable type, the following specific impedances have been measured: L'=0.525 µH/m, R'=5.75 mΩ/m, C'=0.21 nF/m.

Figure 6 shows the structure and parameters of the DC grid at the Fraunhofer Institute IISB in Erlangen with specific cable lengths and measured values for the equivalent RLC circuits. A DC grid stability analysis and characterization of this DCC+G test bed has been performed by the project partner Eindhoven University aiming on a stable DC grid operation [24], [25].

The cable impedance model of this DC test bed is also used for the estimation of voltage drop and power losses in the cables. The longest cable distance in the demonstrator facilities is 81 m to the EV-charger. In the DC case, the rated charging power of 7.6 kW causes a voltage drop along the cable of 9.7 V and losses of 198.3 W (2.6 %) will heat up the cable.

In the case of an AC distribution on the same cable the 7.6 kW input power would cause a voltage drop of 16.9 V and 599.2 W (7.9 %) of losses. These values have been calculated assuming a resistive load behavior of the EV charger ($R_{Load,AC}$ = 5.97 Ω, $I_{Load,AC}$ = 35.65 A), i.e. a power factor of 1. The DC distribution in this EV charging example achieves 5.3 % higher efficiency.

VIII. ARC DETECTION AND DC SWITCHING

The basic structure of the DCC+G office demonstrator grid shows a star architecture. All sub parts are connected to a DC distribution cabinet. Around this star point all the equipment for current and voltage measurement and arc monitoring is installed. A Programmable Logic Controller (PLC) controls and monitors the power flows of each sub-system as shown in figure 7.

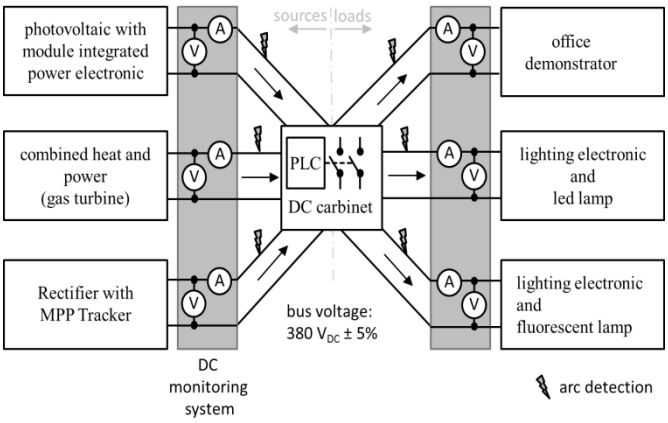

Figure 7: Overview of star topology in DCC+G office demonstrator.

The DC distribution cabinet contains all necessary circuit breakers, mechanical switches and controls to ensure an operation within a safe operating area and to interrupt potential fault currents. This DC cabinet uses available DC switch technologies [26], [27]. Besides mechanical switches new technologies as described in [28] for switching currents up to 5000 A will be evaluated at voltages up to 760 V_{DC}. Such high current switches are needed for example to safely disconnect Li-Ion battery systems.

With power electronic and semiconductor technologies like advanced IGBTs it is possible to switch off without arcing [28]. This leads to reduction in costs and volume of the DC cabinet. Other approaches are using mechanical contacts together with a magnetic field to force the arc into an arcing chamber where it expiries quickly [29].

Several arc detection systems have been included in the test bed to investigate the behavior on different locations within the 380 V_{DC} grid [30]. For evaluation proposes there are several different arc detectors installed in the test bed. They have different parameters and react on different arcing behavior.

It is also possible to combine the arc detection monitor with a DC switch or the corresponding power electronic converter (DC/DC, rectifier, LED driver, etc.). Once an arc is detected, a switch or a power electronic converter can be switched off to expire the arc. After that this tree can connect back to the 380 V_{DC} bus. The duration of this process depends on the DC grid design. A good design enables an on and off switching in less than 10 ms. After several arc detections and returns this part of the grid is put in off state.

With this proposed architecture the arc detection is working like normal circuit breaker in an AC case. The necessary electronic for an arc detection system is already available in the power electronic circuits (voltage and current sensors), so an efficient fast and low cost approach is to include the arc detection as an algorithm in the DC/DC converter controller (e.g. FPGA).

IX. Grounding Concepts

The general standard for grounding concepts is IEC 60364-1 "Low voltage electrical installations". Also ETSI standard EN 301 605 documents the two grounding concepts for 380 V DC grids shown in the figures 8 and 9 [31]. This standard is developed for the application in data centers.

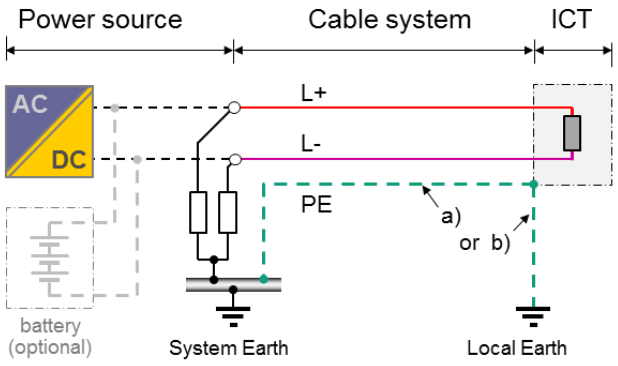

Figure 8: IT system according to ETSI EN 301 605 – Environmental Engineering (EE); Earthing and bonding of 400 VDC data and telecom (ICT) equipment.

An IT system as shown in figure 8 is commonly used in data centers to increase the availability. A connection between one conductor and ground, e.g., does not result in an immediate break of operation.

The traditional building installations are commonly adapted for TN-S. Mixing of IT and TN-S on the same site is not a problem but the management of large area systems in IT is more complex as in TN-S systems.

The DCC+G office test bed at the Fraunhofer Institute IISB will make use of a TN-S system depicted in figure 9.

The used grounding system has also an important impact of the Filter designs.

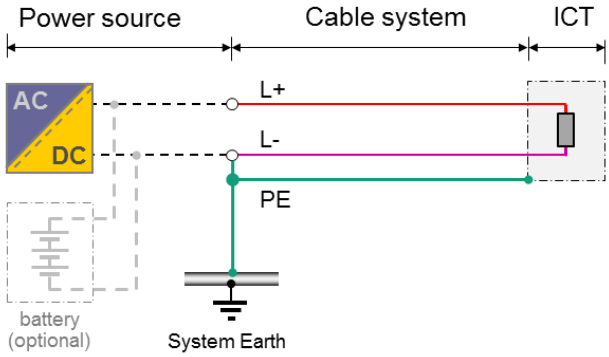

Figure 9: TN-S system according to ETSI EN 301 605 - Environmental Engineering (EE); Earthing and bonding of 400 VDC data and telecom (ICT) equipment.

X. Office Building Demonstration

The validation of the proposed 380 V_{DC} Grid system makes use of a DC test grid at Fraunhofer IISB in Erlangen. The sources and loads of the test grid interface the grid through power electronic components that were developed within the DCC+G project, e. g. the central rectifier (Emerson Network Power), LED driver (Philips), Solar Micro Inverter (Heliox) and the Micro-CHP-unit (MTT), and through commercially available switch mode power supplies which were retrofitted for direct use in a 380 V_{DC} grid environment, e. g. the above discussed fluorescent lamp drivers.

Figure 10: Fraunhofer Institute IISB building AE in Erlangen is the office test bed for proposed 380 V_{DC} grid.

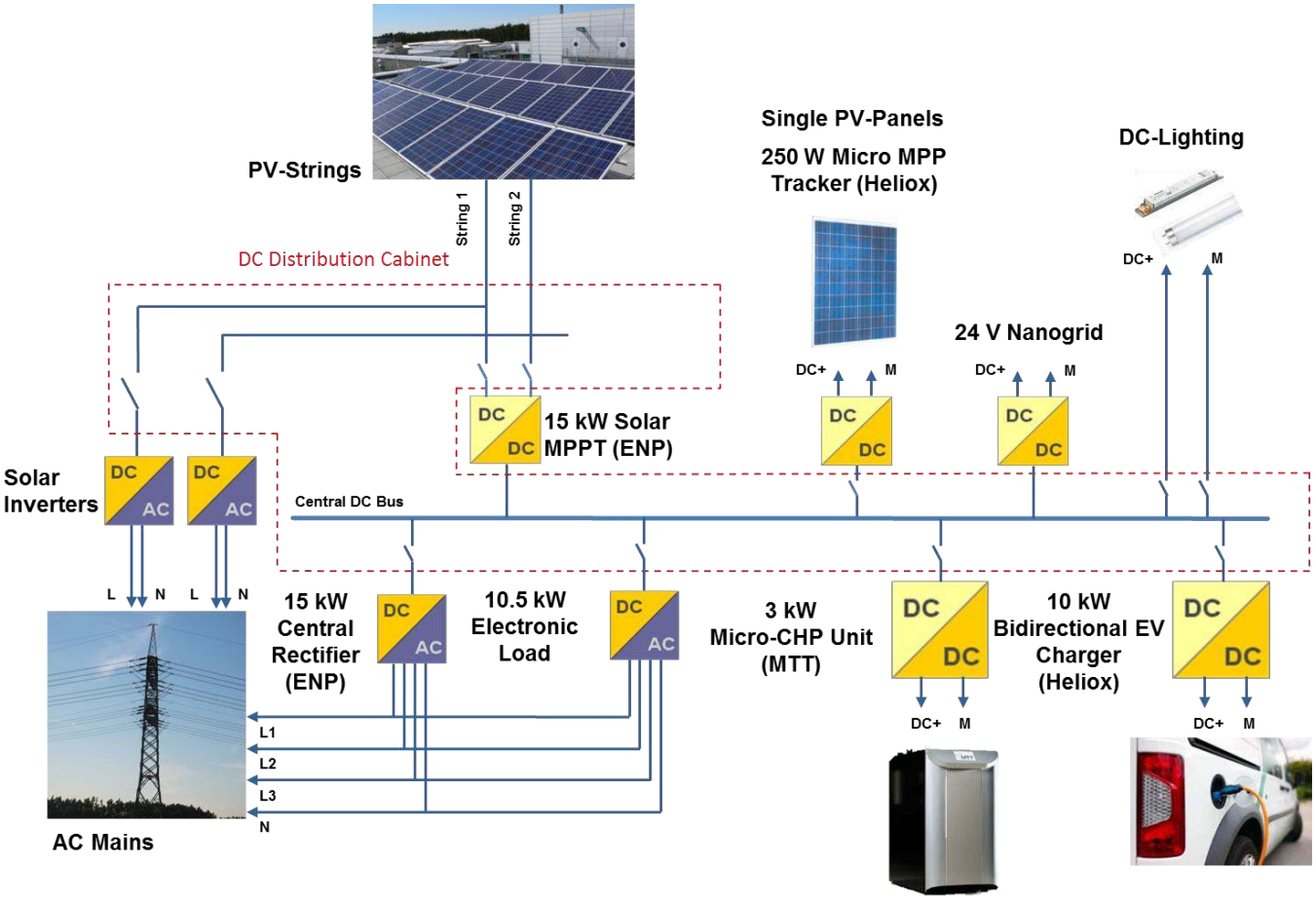

Figure 11: Schematic overview of DCC+G office demonstrator in Fraunhofer Institute IISB in Erlangen.

In figure 10 the PV, EV charging stations, and some distribution parts are shown, a schematic build-up of the test-grid is given in figure 11.

More in detail the test bed is equipped with two DC bus bars, the central 380 V_{DC} bus and a DC bus of the photovoltaic solar panels. The difference between the two buses is that the voltage of the central DC bus is controlled to a nominal value of 380 V_{DC}. A droop control scheme in each power converter connected to this bus ensures keeping the voltage within ± 20 V boundaries of the nominal value. The PV bus, on the other side, has a larger voltage range up to 800 V_{DC} that depends on solar irradiation and the temperature of the solar cells.

For the connection of the PV panels to the central DC bus, two options were realized in the DC test grid in Erlangen:

- The first option is a series and parallel connection of the PV panels to form a string with up to 800 V_{DC}. The maximum power point tracking (MPPT) tracking for the whole string is then executed by an Emerson 15 kW DC/DC MPPT converter which is included in the 15 kW central rectifier cabinet, see figure 12.

- Another option is to use PV panel integrated MPP trackers in the power range of 250 W that will be provided by project partner Heliox BV. These power converters step-up the panel voltage directly to the 380 V_{DC} bus voltage and realize MPP tracking for each panel individually, which is superior to the string connection in case of clouding.

Another source in the DC grid is a Micro-CHP-unit from project partner MTT. This gas turbine based CHP system can deliver up to 10 kW heat and 3 kW electrical power. It is connected to the water cycle of the building so all thermal power can be used in the facility. An integrated DC/DC converter handles connection to the 380 V_{DC} grid. If the bus voltage rises above 385 V_{DC} the MTT system will switch-of automatically and will restart again if the voltage drops below 375 V_{DC}.

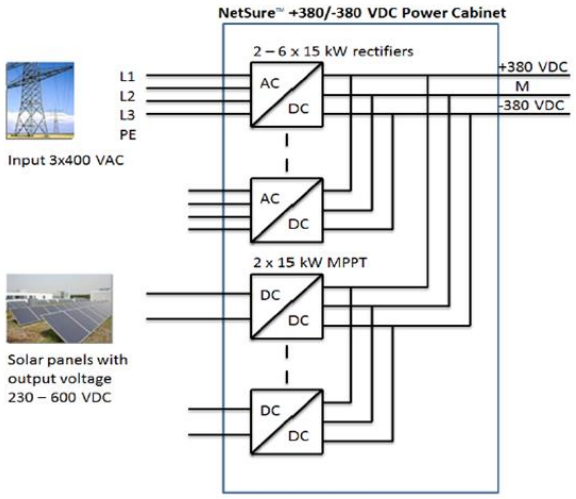

Figure 12: NetSure ±380 V_{DC} power cabinet overview from Emerson Network Power with rectifier and MPPT.

It is also possible to drive the MTT with a strategy based on the heating needs, which will be more suitable in smaller environments. In this test bed the thermal power is small compared to the total heat requirement of the facility, so the MTT is only grid voltage controlled.

As can be seen in figure 13 the lighting grid comprises two strings. One is built with fluorescent lights, the second is equipped with LED lights. This build-up was selected to enable a technology comparison in the context of DC grids. Both lighting grid strings are fed from the central DC bus.

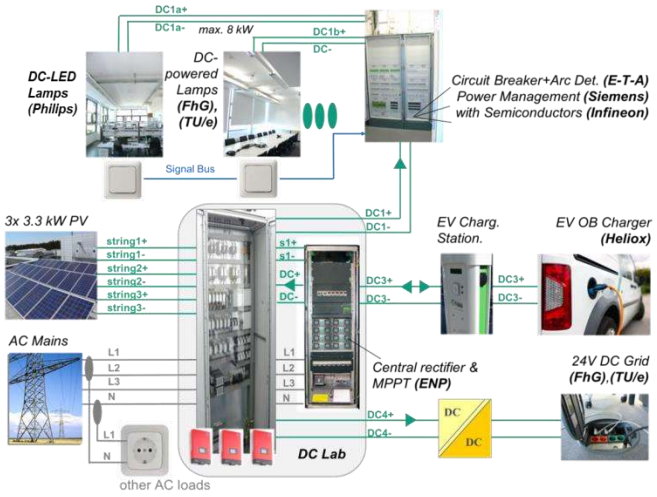

Figure 13: Overview of DC and AC distribution and the developed components usage in DCC+G.

To show the benefits of a direct current power supply for small office devices like laptops, monitors, telephone and USB equipment, these devices are also connected to the 380 V_{DC} bus. This is realized using an isolating 600 W DC/DC converter. Depending on the office equipment (laptop or workstation) this power level is suitable for up to four office workplaces.

It is the same motivation as using the proposed central rectifier concept with the same advantages. The isolating converter for the 380 V_{DC} to 24 V conversion is centralized in each office room. The power supply of the high number of end devices need only a voltage converter to 24 V which is less expensive and volume intensive.

In each room one or more converter supplies a 24 V bus for end devices. It is also planned to use this 24 V bus to supply other systems in the building. The relays in the switching cabinet, control and monitoring devices or the KNX bus can then be supplied out of the 24 V bus.

For all devices which cannot be powered direct with 24 V a further DC/DC converter is used to convert the voltage. This additional converter can be included into the device or be implemented in a plug or desk systems as can be seen in figure 14.

XI. HIGH POWER LOADS

The partners of the DCC+G consortium propose a 2-phase ± 380 V_{DC} grid for higher power levels due to its higher performance compared with a standard 3-phase 230 V / 400 V AC grid.

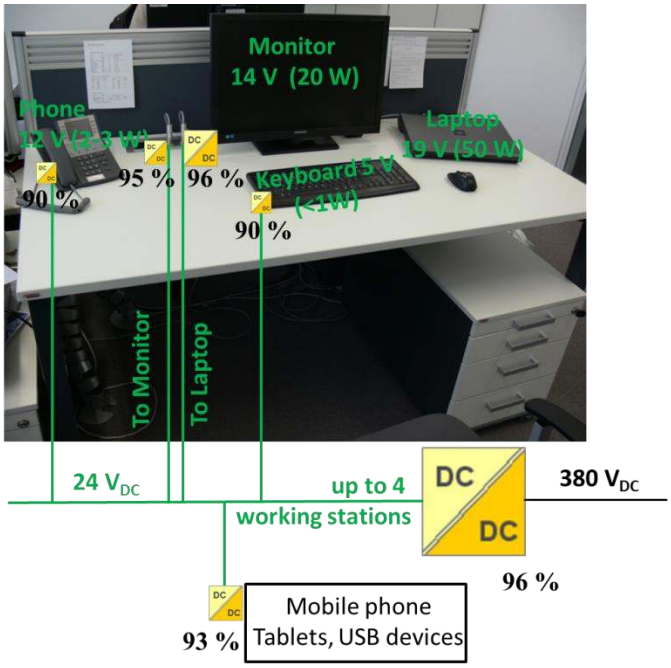

Figure 14: Typical office desk with equipment requiring different voltage levels. Tiny DC/DC converters are integrated into the desk or the plug.

DCC+G partner Emerson Climate Technology is developing a new cooling compressor. Also medium size air-conditioning can benefit from a 2-phase 380 V_{DC} grid. In combination with a rectifier and solar MPP-tracker, as shown in figure 15, this topology can provide savings of up to 5 % compared to an equivalent AC coupled grid. This is described in detail in [32]. Other examples for connecting loads direct to a 2-phase ± 380 V_{DC} grid is a DC charging station for electric vehicles which can have an output voltage up to 850 V_{DC} according to IEC 62196–3.

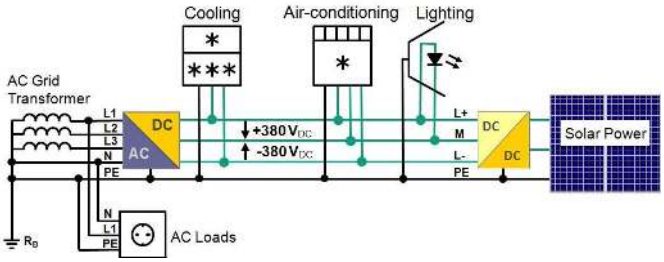

Figure 15: Proposed 2-phase DC-Grid system for high power and high efficiency applications with ±380 V_{DC}

XII. CONCLUSION

With the proposed DC grid approach both an efficiency and availability improvement as well as a reduction of cost and system complexity can be realized.

It is shown that less conversion losses and higher distribution efficiency can be achieved with a 380 V_{DC} grid compared to traditional AC grids. Also higher currents can be distributed over the same existing wire harness. High power loads like air conditioner and cooler can benefit from a connection to a 2-phase ± 380 V_{DC} grid. Further benefits of the proposed grid architecture are less costs and volume through more centralized power electronics which brings scaling benefits.

Also the EMI filter design for DC appliances (e.g. fluorescent/LED lamp driver) has been discussed and the advantages of a filter design for higher frequency and bandwidth are shown. This result in a smaller footprint and less costs compared to the AC case.

ACKNOWLEDGMENT

We thank the Bundesministerium für Bildung und Forschung and the European Community for funding the project DCC+G (BMBF FKZ 13N12113; ENIAC Nr. 296108 “DC Components and Grid”).

REFERENCES

[1] Shenai, K., "Optimized trench MOSFET technologies for power devices," Electron Devices, IEEE Transactions on , vol.39, no.6, pp.1435,1443, Jun 1992.

[2] Lorenz, L., "Fast switching power semiconductor devices and Smart Power IC´s: An enabling technology for future high efficient electronic system," VLSI Technology Systems and Applications (VLSI-TSA), 2010 International Symposium on , vol., no., pp.168,170, 26-28 April 2010.

[3] Gammon, P., "Silicon and the wide bandgap semiconductors, shaping the future power electronic device market," Ultimate Integration on Silicon (ULIS), 2013 14th International Conference on , vol., no., pp.9,13, 19-21 March 2013.

[4] Avron, A., “Super Junction MOSFET”, Technology & Market Report, May 2011.

[5] Reusch, D.; Strydom, J., "Understanding the Effect of PCB Layout on Circuit Performance in a High-Frequency Gallium-Nitride-Based Point of Load Converter," Power Electronics, IEEE Transactions on , vol.29, no.4, pp.2008,2015, April 2014.

[6] Kolar, J.W.; Biela, J.; Waffler, S.; Friedli, T.; Badstuebner, U., "Performance trends and limitations of power electronic systems," Integrated Power Electronics Systems (CIPS), 2010 6th International Conference on , vol., no., pp.1,20, 16-18 March 2010.

[7] Kolar, J.W.; Drofenik, U.; Biela, J.; Heldwein, M.L.; Ertl, H.; Friedli, T.; Round, S.D., "PWM Converter Power Density Barriers," Power Conversion Conference - Nagoya, 2007. PCC '07 , vol., no., pp.P-9,P-29, 2-5 April 2007.

[8] Baliga, B. Jayant, "The future of power semiconductor device technology," Proceedings of the IEEE , vol.89, no.6, pp.822,832, Jun 2001.

[9] “First Device in New Line of 600V Power MOSFETs Establishes Industry Benchmark for Low On-Resistance and Fast Switching Performance”, Renesas, Apr 2011.

[10] März, M.: Intelligente Netz- und Gerätekonzepte für morgen, TEP Oberseminar, TU München, 2014.

[11] Ott, L., “Power Electronics for Low-Voltage DC Grids in Commercial Buildings”, VDE Congress 2014.

[12] Lidow, A.; Strydom, J.; Reusch, D., “GaN – Moving Quickly into Entirely New Markets,” Power Electronics Europe, Issue 4, 2014.

[13] Reusch, David; Strydom, Johan, "Improving Performance of High Speed GaN Transistors Operating in Parallel for High Current Applications," PCIM Europe 2014; International Exhibition and Conference for Power Electronics, Intelligent Motion, Renewable Energy and Energy Management; Proceedings of , vol., no., pp.1,8, 20-22 May 2014.

[14] Strydom, J.; Reusch, D., "Design and evaluation of a 10 MHz gallium nitride based 42 V DC-DC converter," Applied Power Electronics Conference and Exposition (APEC), 2014 Twenty-Ninth Annual IEEE, vol., no., pp.1510,1516, 16-20 March 2014.

[15] ETSI EN 300 132-3-1 - Environmental Engineering (EE); Power supply interface at the input to telecommunications and datacom (ICT) equipment; Part 3: Operated by rectified current source, alternating current source or direct current source up to 400 V; Sub-part 1: Direct current source up to 400 V, European Standard EN 300 132-3-1 V2.1.1 (2012-02)

[16] Isaac Cohen and Bing Lu, “High Power Factor and High Efficiency—You Can Have Both,” TI Power Supply Design Seminar, SEM1800, Sep 2008.

[17] Becker, D.J.; Sonnenberg, B. J., "400Vdc power distribution: Overcoming the challenges," Telecommunications Energy Conference (INTELEC), 32nd International , vol., no., pp.1,10, 6-10 June 2010.

[18] Bolla, R. , Bruschi, R., D’Agos, L., “An Energy-aware Survey on Mobile-Phone Chargers”, 2011

[19] CISPR 15 ed8.0, “Limits and methods of measurement of radio disturbance characteristics of electrical lighting and similar equipment”, IEC, 2013.

[20] Chow, AC.; Perreault, D.J., "Active EMI filters for automotive motor drives," Power Electronics in Transportation, 2002 , vol., no., pp.127,134, 24-25 Oct. 2002

[21] Nalborczyk, J.N., “Shortcomings of Simple EMC Filters”, MPE Ltd., Liverpool, EMC Directory & Design Guide, 2012.

[22] Boeke U.; Weiss R.; Mauder A.; Hamilton L.; Ott, L., "Efficiency Advantages of ±380 V DC Grids in Comparison with 230 V/400 V AC Grids". DCC+G White Paper. 2014 Available: http://dcgrid.tue.nl/files/2014-05-05_DCC+G-White_Paper_Efficiency_Advantages_of_DC_Power_Grids_v1-0.pdf (Accessed 22 July 2014)

[23] “Metals mired in global uncertainty - Gold, silver and copper price report 2014”, PWC, 2014.

[24] K. Rykov, J.L. Duarte, M. Szpek, J. Olsson, S. Zeltner, and L. Ott "Converter Impedance Characterization for Stability Analysis of Low-Voltage DC-Grids". IEEE PES Conference on Innovative Smart Grid Technology ISGT 2014

[25] Rykov, K.; Duarte, J.L.; Boeke, U.; Wendt, M.; Weiss, R., "Voltage stability assessment in semi-autonomous DC-grids with multiple power modules," Power Electronics and Applications (EPE), 2013 15th European Conference on , vol., no., pp.1,10, 2-6 Sept. 2013

[26] “DC rated switch-disconnectors OTDC 16 to 32 Amperes”, Technical article, ABB, 2011

[27] Schaltbau , „Schütze CT1115/04, CT1130/04, CT1115/08, CT1130/08 1-polige Leistungsschütze für AC und DC Katalog C20.de“, Germany, 2013

[28] Meckler, Peter; Gerdinand, Frank; Weiss, Roland; Boeke, Ulrich; Mauder, Anton, "Hybrid switches in protective devices for low-voltage DC grids at commercial used buildings," ICEC 2014; The 27th International Conference on Electrical Contacts; Proceedings of , vol., no., pp.1,6, 22-26 June 2014

[29] Vassa, A; Carvou, E.; Rivoirard, S.; Doublet, L.; Bourda, C.; Jeannot, D.; Ramoni, P.; Ben Jemaa, N.; Givord, D., "Magnetic Blowing of Break Arcs up to 360 VDC," Electrical Contacts (HOLM), 2010 Proceedings of the 56th IEEE Holm Conference on , vol., no., pp.1,5, 4-7 Oct. 2010

[30] Strobl, Christian, "Arc Fault Detection - a Model-based Approach," ICEC 2014; The 27th International Conference on Electrical Contacts; 22-26 June 2014

[31] ETSI EN 301 605 - Environmental Engineering (EE); Earthing and bonding of 400 VDC data and telecom (ICT) equipment

[32] Boeke, U.; Ott, L., "Impact of a ±380 V DC Power Grid Infrastructure on Commercial Building Energy Profiles". DCC+G White Paper. [Online]. Available: http://dcgrid.tue.nl/files/2014-04-28_DCC+G-White_Paper-Building_profiles_and_impact_by_DC_grids.pdf (Accessed 22 July 2014)